Supporting information for: Fast quantitative single-molecule detection at ultralow concentrations

- Supporting Information -

Philippe Haas,[†,@] Patrick Then,[‡,@] Andreas Wild,[†,@] Wilfried Grange,[¶] Sylvain Zorman,[¶] Martin Hegner,[§] Michel Calame,[‖] Ueli Aebi,[⊥] Josef Flammer,[#] and Bert Hecht[*,‡]

National Center of Competence for Research in Nanoscale Science (NCCR), Institute of Physics, Klingelbergstr. 82, CH-4056 Basel, Switzerland, Nano-Optics & Biophotonics Group, Physikalisches Institut, Wilhelm-Conrad-Röntgen-Center for Complex Material Systems (RCCM), Experimentelle Physik 5, Am Hubland, 97074 Würzburg, Germany, Institut Jacques Monod, 15 rue Hélène Brion, 75013 Paris, France, Centre for Research on Adaptive Nanostructures and Nanodevices, College Green, Dublin 2, Ireland, Klingelbergstrasse 82, CH-4056 Basel, Switzerland, Klingelbergstrasse 50-70, CH-4056 Basel, Switzerland, and Mittlere Strasse 91, CH-4031 Basel, Switzerland

E-mail: hecht@physik.uni-wuerzburg.de

[*]To whom correspondence should be addressed
[†]NCCR, University of Basel
[‡]Universität Würzburg
[¶]Université Paris 7 et CNRS
[§]Trinity College Dublin
[‖]Department of Physics, University of Basel
[⊥]Biozentrum, University of Basel
[#]Universitätsaugenklinik, University of Basel
[@]authors contributed equally, alphabetical order

Supporting Information 1

Approximation of first passage time

For a concentration-independent diffusion coefficient D, Fick's (second) law states

$$\frac{\partial c}{\partial t} = D\nabla^2 c \tag{1}$$

Assuming the detection volume to be a sphere of radius a and rewriting 1 using spherical coordinates yields

$$\frac{\partial c}{\partial t} = D\frac{1}{r^2}\frac{\partial}{\partial r}\left(r^2\frac{\partial c}{\partial r}\right) . \tag{2}$$

For the stationary case this equation reads as

$$\frac{\partial c}{\partial t} = 0 . \tag{3}$$

We now assume that the concentration within the detection volume is zero at any given time (i.e. once a molecule enters the detection volume, it is instantly bleached) and that the concentration is c_0 for $r >> a$. The concentration can then be written as

$$c(r) = c_0\left(1 - \frac{a}{r}\right) . \tag{4}$$

Fick's first law can be used to calculate the diffusive flux J driven by a concentration gradient

$$J(a) = -D\frac{\partial c}{\partial r} \tag{5}$$

Calculating the total flux we get

$$J = 4\pi a D c_0 \tag{6}$$

which can be used to estimate the total number of molecules reaching the sphere during the time t by $J \times t$. The probability $P(k,\lambda)$ that there are k occurrences for an expected number of λ

occurrences during the time interval t is given by the Poisson distribution

$$P(k,Jt) = \frac{e^{-Jt}(Jt)^k}{k!} \; . \tag{7}$$

The average time it takes to observe a molecule corresponds to the average time for which no molecule is in the detection volume. The probability for zero molecules in a time interval t is

$$P(0,Jt) = e^{-Jt} \; . \tag{8}$$

The average time therefore reads as

$$< t >= \frac{1}{\int_0^\infty P(0,Jt)dt} \cdot \int_0^\infty tP(0,Jt)dt = \frac{1}{4\pi aDc_0} \; . \tag{9}$$

In Figure 1 9 is used to calculate the average time it takes until a molecule reaches a 10 fl volume for different values of the diffusion coefficient D. For bigger molecules reasonable values for D range between $1 \cdot 10^{-10} m^2/s$ and $5 \cdot 10^{-10} m^2/s$. For this case, single molecule detection by diffusion will be limited to concentrations above roughly 10 fmol/l, as for lower concentrations the average time until a molecule will be detected quickly reaches several tens of minutes to hours.

Methods

The complete experimental setup is depicted in Figure 2. A semiconductor-diode-laser (**L**, IDT0-635-30, GMP, 30 mW) emitting at 635 nm is providing the excitation light. After passing through a filter wheel to control the power, the laser beam is deflected by a dichroic mirror (**1**, T740/140 650 dcip, Chroma) and coupled into a short (20 to 30 cm) piece of single-mode optical fiber (**F**, FS-SN-3224, λ_{cutoff}=630 nm and FS-SN-4224, λ_{cutoff}=820 nm; Thorlabs). Fibers have been chosen for low Raman background. The light is transmitted through the fiber and emitted via a 90^o-cleaved fiber end into the liquid sample volume **P**, where it excites single molecules whose

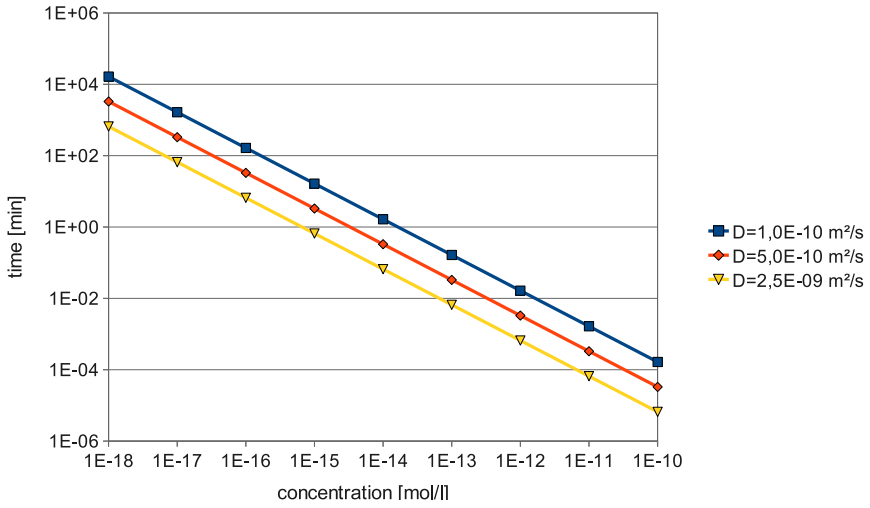

Figure 1: Average time until a molecule enters a 10 fl detection volume using equation 9. The diffusion coefficient has been chosen as $D = 1 \cdot 10^{-10} m^2/s$ (squares), $D = 5 \cdot 10^{-10} m^2/s$ (diamonds) and $D = 2,5 \cdot 10^{-9} m^2/s$ (triangles), respectively.

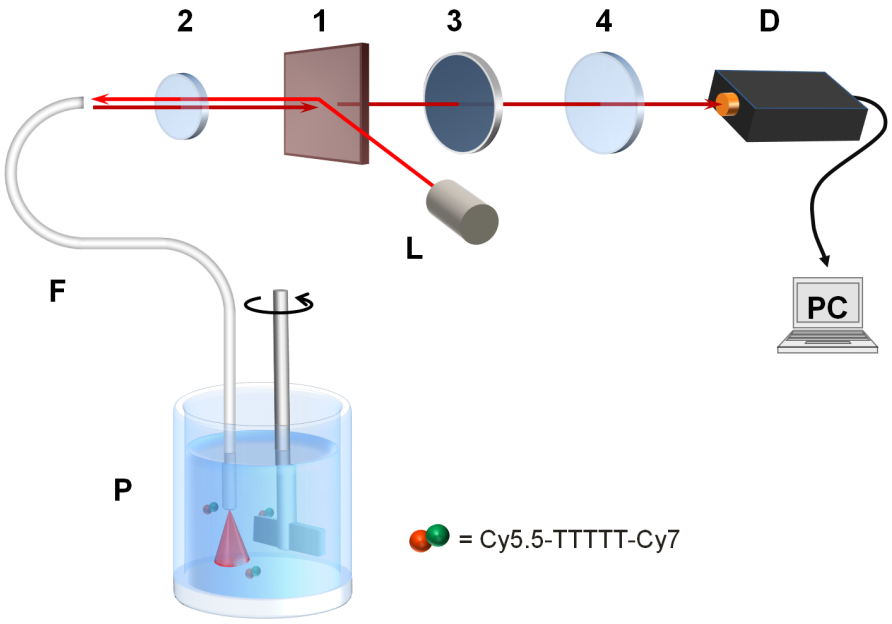

Figure 2: Schematic diagram of the experimental setup. L: Diode laser, 1: Dichroic mirror, 2: Microscope objective for fiber coupling, F: Short piece of single-mode optical fiber (20-30 cm), P: Sample container (ø=10 mm,V=1 ml), 3: Bandpass filter, 4: Focusing lens, D: single-photon counting avalanche photodiode module.

fluorescence is coupled back into the fiber with sufficiently high efficiency. The fiber is connected to a computer controlled *xyz* positioner (I3005, Luminos Industries) which allows for a precise positioning of the fiber relative to the rotor. Best results were obtained when the fiber was slightly tilted into or out of the flow direction by $\sim$ 5-10°. All experiments were carried out using small concentrations of dye molecules dissolved in a buffer solution (10 mM TRIS-HCl, 50 mM KCl and 1.5 mM $MgCl_2$ in water, pH of 8.3). Wavelength-shifted single-molecule fluorescence after exiting the fiber passes the dichroic mirror, while residual excitation light traveling backwards through the fiber or being reflected at the fiber end facet gets deflected. The remaining light passes a bandpass filter (**3**, XF3307, Omega Optical) and is focused by a convex lens (**4**, f=30 cm) onto the active area (ø=180 μm) of a single photon counting avalanche diode (**D**, SPCM-AQR-13, Perkin Elmer, quantum efficiency at 780 nm $\approx$ 60 %) whose output is fed into a PC and evaluated by counting fluorescence bursts in the fluorescence time traces using a custom-made software (Labview, National Instruments) as described in **Supporting Information 5**. The focal length has been chosen such that the image of the fiber core fits the active area of the detector thus preventing excess background originating from cladding modes from reaching the detector's active area.

Supporting Information 2

Detection efficiency

The detection efficiency of the setup is dominated by the collection efficiency of the optical fiber. To calculate the percentage of light emitted by a dye molecule that is coupled into the fiber, we model an electric dipole close to a plane interface between two dielectric media (water: $n_1 = 1.33$ and glass: $n_2 = 1.54$). As the parallel orientation to the plane interface has a much higher statistical weight as opposed to the perpendicular orientation, we limit our analysis to parallel oriented dipoles. For a detailed analysis, the interested reader is referred to[1] and[2]. Here we only present the results of the calculation.

If a dipole is located close to a plane interface between two dielectric media of different index

of refraction, the majority of the dipole emission will be coupled into the higher refractive index material. However, for an optical fiber, only the fraction of light entering the fiber up to the critical angle for total internal reflection within the fiber will couple to the fibers' guided mode. This angle can be calculated using the numerical aperture $NA = n \cdot sin(\theta_1)$ of the optical fiber. By using Snell's law we find the maximum angle for light to be transported through the fiber by total internal reflection:

$$sin(\theta_2) = \frac{1}{n_2} \cdot NA \; . \tag{10}$$

Therefore, for NA=0.12, only light that is propagating in the fiber with a maximum angle of $\pm$ 4.47° can be transported through the fiber. This yields a fraction of 0.3% of the light emitted by a molecule. It should be noted that this value is independent of the distance of the dipole to the plane interface, as the distance affects only the amount of evanescent waves coupled into the second medium. However, as the equation used to calculate the emission pattern assumes an infinite plane, it is to be expected that the results are valid only for molecules sufficiently close to the interface. Furthermore, the molecules have to be close to the core of the fiber. Both factors limit the detection volume to approximately 10 femtoliters. Neglecting comparably minor losses in the lenses and the dichroic mirror, additional losses mostly occur at the bandpass-filter (transmission $\sim$ 80 %) and at the detector (quantum yield at 780 nm $\sim$ 60%). Consequently, the total detection efficiency is estimated to $\sim$ 0.15 %.

Supporting Information 3

FRET dyes

The dyes used in this work were Cy5.5 and Cy7, a well-known FRET, pair linked by 5 thymidine bases (Cy5.5-TTTTT-Cy7). The thymidine bases have been chosen because they exhibit low quenching of the fluorescence emission[3,4]. Figure 3 shows normalized spectra of the light leaving the fiber together with the transmission curve of the bandpass filter. The bandpass filter is matched to the emission band of Cy7. The spectrum of the background was recorded with the fiber

end in air, while the spectra of Cy5.5 and Cy7 were recorded when dipping the fiber in solutions containing sufficiently large concentrations of the pure dyes. Using a bandpass filter with high transmission around 800 nm largely suppresses the background generated in the fiber while transmitting most of the acceptor fluorescence. A main advantage of the Cy5.5-Cy7 pair is the acceptor emission in the NIR spectral range, as few naturally occurring compounds emit light in this range.

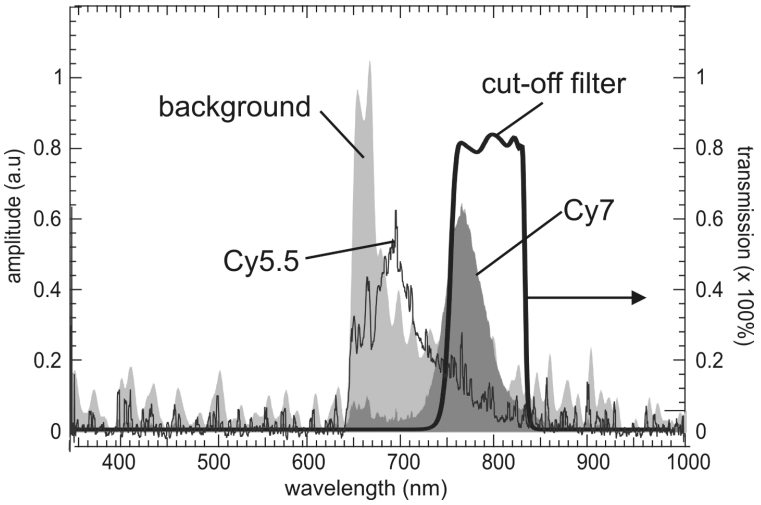

Figure 3: Spectra of light leaving the fiber towards the detector. As indicated: Spectrum of the background caused by inelastic scattering of the excitation light in the optical fiber as well as the fluorescence emission of solutions of Cy5.5 and Cy7 as well as the transmission spectrum of the bandpass filter (see Figure 2, **3**, XF3307, Omega Optical). The sharp cutoff towards shorter wavelength in the background as well as the Cy5.5 fluorescence spectrum at $\approx$ 640 nm is due to a notch filter centered at 632 nm.

Supporting Information 4

Position optimization

Since the velocity profile in the analyte solution varies as a function of the distance to the rotor, we expect the detection rate of the setup to be strongly dependent both on the stirring rate of the rotor and on the fiber position relative to the rotor. Therefore, to optimize the detection rate, an optimal fiber position and stirring rate has been determined. To this end, series of 30 s time traces have been recorded at different axial and radial positions of the fiber at a fixed stirring rate of 20000 rpm. After each measurement the fiber was moved by 50 μm to a new position. Figure 4 shows the result

of the radial (x) variation of the fiber position. Coordinates have been determined by measuring the distance to the upper corner of the rotor, counting outwards (see inset in Figure 4). A maximum in the number of counted bursts is found at a fiber position of 0.45 mm when moving from 0.6 mm to 0.05 mm and at a fiber position of 0.35 mm when moving back, respectively. Accordingly, a position of x= 0.4 mm has been chosen for all subsequent measurements. The optimal position in axial (y) direction has been determined in similar experiments. A set of measurements has been performed changing the height of the fiber in steps of 200 μm. A maximum is found at a position of 0.3 mm as seen in figure Figure 4. Accordingly, for subsequent measurements a position of y= 0.3 mm has been chosen. In comparison to the radial fiber scan, the y-scan is much broader. Therefore the vertical position of the fiber can be considered not to be as critical for optimal detection. In similar experiments, time traces have been recorded for different stirring rates but at fixed radial and vertical position. At stirring rates above ≈16000 rpm the number of detected molecules begins to saturate (see Figure 5). A rate of 20000 rpm, well within saturation, has therefore been chosen for the experiments. We have also performed an autocorrelation analysis of time traces recorded at different stirring speed (1 pM concentration) which shows increasing burst width for increasing stirring speed indicating the formation of vortices. The results are displayed in Fig. Figure 5 (b)

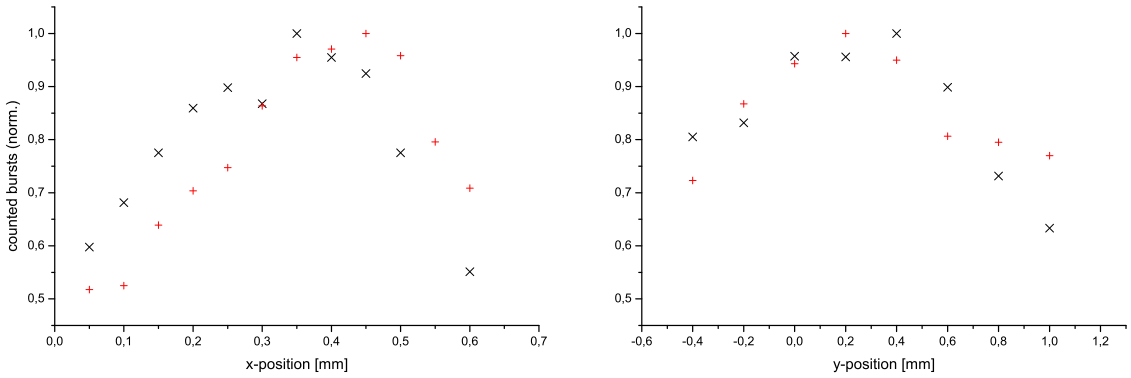

Figure 4: Dependence of the number of fluorescence bursts on the radial fiber position (left) and vertical fiber position (right). The position is determined outwards from the edge of the rotor. (+) has been measured form high to low values, (x) from low to high values.

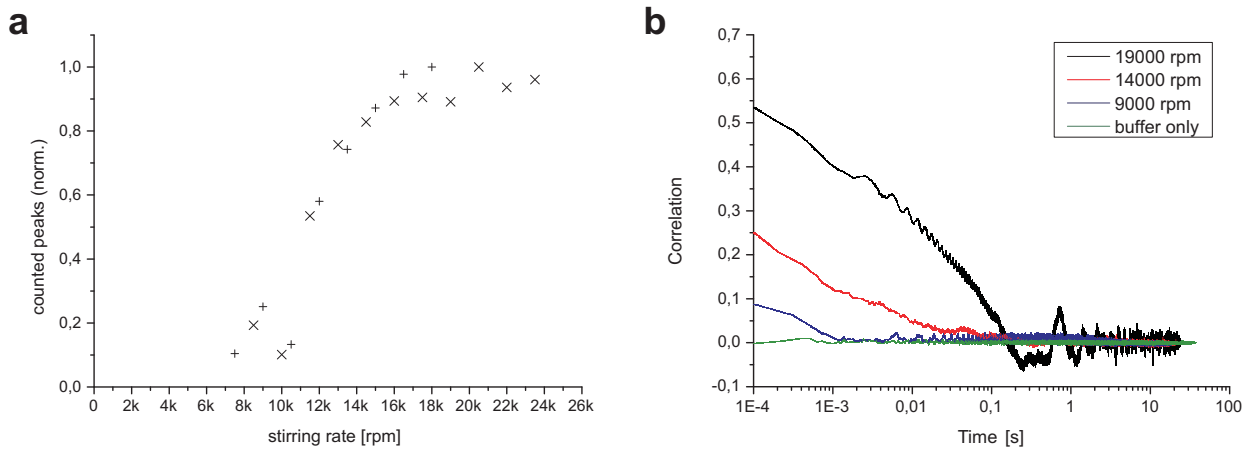

Figure 5: **a**:Dependence of detected molecules on the stirring rate at fixed position. (+) has been measured form high to low values, (x) from low to high values.**b**: Autocorrelation of time traces recorded at 1 pM concentration showing increasing fluorescence burst width for increasing stirring rates indicating the formation of vortices.

Supporting Information 5

Data analysis

The recorded time traces are evaluated using a burst-detection and counting algorithm described in Grange et al.[5]. In brief, the algorithm distinguishes between the distribution of the burst histogram and the distribution of the background by directly using the time-trace including all single-molecule bursts to obtain a first guess to describe the background alone. Every burst above a certain, predefined threshold χ is then counted and subsequently removed from the time trace using a routine implemented in Labview (National Instruments). In the next iteration, the time-trace - now without the previously detected bursts - is again used to determine an already much better estimate for the background distribution. These steps are repeated until all bursts have been counted and the background distribution is not improved any more by removing more bursts. An important factor is the threshold χ that defines the allowed overlap between the background and the burst distributions. For low χ, few (down to <1) wrong positive bursts will be detected, inevitably leading to some amount of signal bursts in the overlap region of the two distributions to be missed. A higher χ results in the detection of more bursts, but also some wrong positive (background) bursts will be

detected, which depending on the application, may however be tolerable. Prior to evaluating the experimental data, therefore a value for the threshold χ has to be chosen. By analyzing a typical data set for different values of χ, a value of 400 was found to be a reasonable choice for all but the smallest concentrations investigated in the present study. At this value, the root mean squared error (RMSE), providing an estimate of the quality of the fit to the resulting Poissonian background distribution with all bursts removed, is significantly reduced while the number of detected bursts considerably increased. At the same time the number of wrong positives stays comparatively low. For further details see[5].

References

(1) Lukosz, W.; Kunz, R. *J. Opt. Soc. Am.* **1977**, *67*, 1615–1619.

(2) Novotny, L.; Hecht, B. *Principles of Nano-Optics*; Cambridge University Press, 2006.

(3) Seidel, C. A. M.; Schulz, A.; Sauer, M. H. M. *The Journal of Physical Chemistry* **1996**, *100*, 5541–5553.

(4) Tyagi, S.; Marras, S.; Kramer, F. *Nucleic Acids Research* **2002**, *30*, e122.

(5) Grange, W.; Haas, P.; Wild, A.; Calame, M.; Hegner, M.; Hecht, B. *J. Phys. Chem. B* **2008**, *112*, 7140–7144.